Journal of Physics: Conference Series

PAPER • **OPEN ACCESS**

Efficient operation of anisotropic synchronous machines for wind energy systems

To cite this article: Hisham Eldeeb *et al* 2016 *J. Phys.: Conf. Ser.* **753** 112009

Efficient operation of anisotropic synchronous machines for wind energy systems

Hisham Eldeeb[†], **Christoph M. Hackl**[†,⋆] **and Julian Kullick**[†]

[†]All authors (in alphabetical order) contributed equally to this paper; [⋆]Corresponding author
Research group "Control of Renewable Energy Systems (CRES)"
Munich School of Engineering, Technical University of Munich, 85748 Garching, Germany

E-mail: hisham.eldeeb@tum.de, christoph.hackl@tum.de[⋆], julian.kullick@tum.de

Abstract. This paper presents an *analytical* solution for the Maximum-Torque-per-Ampere (MTPA) operation of synchronous machines (SM) with *anisotropy* and *magnetic cross-coupling* for the application in wind turbine systems and airborne wind energy systems. For a given reference torque, the analytical MTPA solution provides the optimal stator current references which produce the desired torque while minimizing the stator copper losses. From an implementation point of view, the proposed analytical method is appealing in terms of its fast online computation (compared to classical numerical methods) and its efficiency enhancement of the electrical drive system. The efficiency of the analytical MTPA operation, *with* and *without* consideration of cross-coupling, is compared to the conventional method with zero direct current.

Nomenclature

$\mathbb{N}, \mathbb{R}, \mathbb{C}$ are the sets of natural, real, and complex numbers. $x \in \mathbb{R}$ or $x \in \mathbb{C}$ is a real or complex scalar. $\boldsymbol{x} \in \mathbb{R}^n$ (bold) is a real valued vector with $n \in \mathbb{N}$. $\boldsymbol{X} \in \mathbb{R}^{n\times m}$ (capital bold) is a real valued matrix with $n \in \mathbb{N}$ rows and $m \in \mathbb{N}$ columns. $\boldsymbol{x}_\mathrm{s}^k = (x_s^d,\, x_s^q)^\top \in \mathbb{R}^{n\times m}$ is a stator space vector expressed in the synchronously rotating k-coordinate system (with orthogonal axes known as the *direct (d)* and *quadrature (q)* axes) and may represent voltage, current or flux linkage.

1. Introduction

For wind turbine systems (WTS), the optimal choice for the generator (electrical machine) adopted is still controversially discussed [1]. Doubly-fed induction machines (DFIMs) were considered one of the favourable choices for WTS, owing to their accompanied cost effective power converters and simple control of active/reactive power [2]. However, the depletion of DFIMs with respect to synchronous machines (SMs) became more pronounced due to three reasons: (i) partially rated power converters of DFIMs offer a rather poor voltage ride through capability [3, 4], (ii) SMs do not have slip rings (i.e. lower maintenance), eliminate the need for a gearbox (or allow for a drastic reduction of the gear ratio), have a simpler terminal wiring, and offer better grid support capabilities, and (iii) the increased calls for energy-efficient drives discriminates between SMs and DFIMs [5]. Particular interest has been set to permanent magnet SMs (PMSMs) and PM-excited reluctance SMs (PME-RSMs) [6], since they possess lower electrical losses than DFIMs due to the absence of the copper losses in the rotor. In general, for all WTS topologies such as large-scale or small-scale WTSs or airborne wind energy systems (AWESs), the selected SMs must be robust, cheap, and, most importantly, *efficient*. For pumping-mode AWESs [7, Ch. 2 & 3], the SM will operate in generator *and* also motor mode. Albeit PM machines can be controlled to operate at high power factor [5], this does not necessarily imply that the electrical losses within the adopted SM are minimised [8]. Thus, an optimal control strategy for the SMs is vital to fully realize its intrinsic efficiency. For PMSMs or PME-RSMs, the quadrature-axis stator current i_{s}^{q} is proportional to the produced electromagnetic torque m_{m} if the direct-axis stator current i_{s}^{d} is set to zero. However, in most cases, the electromagnetic torque is a nonlinear function of *both* stator currents [6, 9–11]. Therefore, for a given reference torque $m_{\mathrm{m,ref}}$, optimal stator current references $i_{\mathrm{s,ref}}^{d}$ and $i_{\mathrm{s,ref}}^{q}$ must be computed (see Fig. 1). These optimal current references allow for reduced stator copper losses and higher efficiencies than conventional methods with $i_{\mathrm{s,ref}}^{d} = 0$ [10, 11]. Typically, (i) *magnetic cross-coupling* between the d- and q-axes is *neglected* (even though it has a direct effect on the machine torque; see (4) or [9, 10]) and (ii) *numerical solutions* are employed to compute the optimal references [12].

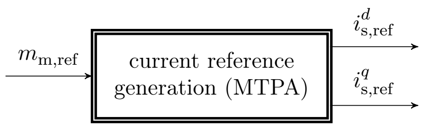

Figure 1: *Generation of the optimal current references with analytical solution* (1).

In [12], optimal feedforward torque control—known as Maximum-Torque-per-Ampere (MTPA)—was suggested by formulating an optimisation problem where a reference current vector with minimal magnitude was computed numerically, which in turn due to the anisotropy gives a noticeable efficiency increment compared to the conventional $i_{\mathrm{s,ref}}^{d} = 0$ approach [13]. For high speeds, further efficiency enhancements can be achieved by considering the iron losses in the machine as well [9, 14]. However, modelling of iron losses is not straight forward (e.g. requires finite element analyses [9]) and, due to the rather low mechanical speeds in WTS, iron losses can be neglected [10]. Nevertheless, solving the MTPA optimisation problem requires nonlinear solvers such as the bisection method (known for its numerical stability but its poor convergence rate [12]) or the Newton-Raphson method (known for its fast convergence but its rather weak numerical stability depending on the initial condition [12]). Moreover, those solvers impose a rather high computational burden on the fixed-point processors adopted for such drives. Only very few results exist which compute an analytical solution to the MTPA optimization problem. In [8] and [15], an analytical expressions for the optimal d-axis reference current (the q-axis reference current comes from the outer speed control loop) has been presented, but magnetic cross-coupling and its impact on the electromagnetic torque were neglected.

In this paper, an *analytical solution for the MTPA optimization problem considering magnetic cross-coupling (i.e. a non-zero mutual inductance* $L_{\mathrm{m}} \neq 0$*)* is presented which allows to compute the optimal d- and q-axis current references

$$\boxed{\boldsymbol{i}_{\mathrm{s,ref}}^{k} = (i_{\mathrm{s,ref}}^{d},\, i_{\mathrm{s,ref}}^{q})^{\top} = \mathrm{MTPA}(m_{\mathrm{m,ref}}, L_{\mathrm{m}}, \ldots, \text{other machine parameters})} \quad (1)$$

online based on the machine parameters and a given (feasible[1]) reference torque $m_{\mathrm{m,ref}}$. The presented method, derived from Lagrangian optimization, is applicable to PMSMs, PME-RSMs or electrically-excited SMs (EESMs) with non-negligible anisotropy and magnetic cross-coupling. Due to space limitations, in the remainder of the paper, only the derivation for permanent-magnet synchronous machines (PMSMs) is shown and discussed.

2. MTPA with analytical solution for PMSMs with magnetic cross-coupling

In this section, the main result of the paper is derived based on the dynamical model of anisotropic PMSMs with magnetic cross-coupling. The result emanates from a Lagrangian formalization of the problem and invoking *Ferrari's method* to solve quartic polynomials [16].

[1] It is assumed that the currents can actually produce the desired reference torque within the electrical drive system; e.g. voltage constraints/maximum-torque-per-volt (MPTV) are not considered.

2.1. Dynamical model of anisotropic PMSMs with magnetic cross-coupling

The generic model of an anisotropic PMSM in the $k = (d, q)$-reference frame is given by [17]

$$\left.\begin{aligned}
&\overbrace{\begin{pmatrix} u_\mathrm{s}^d(t) \\ u_\mathrm{s}^q(t)\end{pmatrix}}^{=:\boldsymbol{u}_\mathrm{s}^k(t)} = R_\mathrm{s} \overbrace{\begin{pmatrix} i_\mathrm{s}^d(t) \\ i_\mathrm{s}^q(t)\end{pmatrix}}^{=:\boldsymbol{i}_\mathrm{s}^k(t)} + n_\mathrm{p}\omega_\mathrm{m}(t) \overbrace{\begin{bmatrix} 0 & -1 \\ 1 & 0\end{bmatrix}}^{=:\boldsymbol{J}} \overbrace{\begin{pmatrix} \psi_\mathrm{s}^d(t) \\ \psi_\mathrm{s}^q(t)\end{pmatrix}}^{=:\boldsymbol{\psi}_\mathrm{s}^k(t)} + \tfrac{\mathrm{d}}{\mathrm{d}t}\boldsymbol{\psi}_\mathrm{s}^k(t), && \boldsymbol{\psi}_\mathrm{s}^k(0) = \boldsymbol{\psi}_\mathrm{pm}^k \in \mathbb{R}^2 \\
&\tfrac{\mathrm{d}}{\mathrm{d}t}\omega_\mathrm{m}(t) = \tfrac{1}{\Theta}\Big(m_\mathrm{m}\big(\boldsymbol{i}_\mathrm{s}^k(t)\big) + \tfrac{m_\mathrm{t}(t)}{g_\mathrm{r}} - \nu_\mathrm{f}\omega_\mathrm{m}(t)\Big), && \omega_\mathrm{m}(0) = \omega_\mathrm{m}^0 \in \mathbb{R} \\
&\tfrac{\mathrm{d}}{\mathrm{d}t}\phi_\mathrm{m}(t) = \omega_\mathrm{m}(t), && \phi_\mathrm{m}(0) = \phi_\mathrm{m}^0 \in \mathbb{R}
\end{aligned}\right\} \quad (2)$$

with stator voltages $\boldsymbol{u}_\mathrm{s}^k = (u_\mathrm{s}^d, u_\mathrm{s}^q)^\top$ (in V^2; e.g. applied by a voltage source inverter), stator currents $\boldsymbol{i}_\mathrm{s}^k = (i_\mathrm{s}^d, i_\mathrm{s}^q)^\top$ (in A^2), flux linkages $\boldsymbol{\psi}_\mathrm{s}^k = (\psi_\mathrm{s}^d, \psi_\mathrm{s}^q)^\top$ (in Wb^2), stator resistance R_s (in Ω), number of pole pairs n_p, mechanical angle ϕ_m (in rad) and speed ω_m (in $\frac{\mathrm{rad}}{\mathrm{s}}$), inertia Θ (in $\mathrm{kg\,m}^2$), machine torque m_m and turbine torque m_t (both in $\mathrm{N\,m}$), gear ratio g_r and viscous friction coefficient ν_f (in $\frac{\mathrm{N\,m\,s}}{\mathrm{rad}}$). The stator flux linkage vector

$$\boldsymbol{\psi}_\mathrm{s}^k(t) = \underbrace{\begin{bmatrix} L_\mathrm{s}^d & L_\mathrm{m} \\ L_\mathrm{m} & L_\mathrm{s}^q \end{bmatrix}}_{=:\boldsymbol{L}_\mathrm{s}^k = (\boldsymbol{L}_\mathrm{s}^k)^\top > 0} \boldsymbol{i}_\mathrm{s}^k(t) + \underbrace{\begin{pmatrix} \psi_\mathrm{pm} \\ 0 \end{pmatrix}}_{=:\boldsymbol{\psi}_\mathrm{pm}^k} \quad (3)$$

is assumed to be an affine[2] function of the stator current vector $\boldsymbol{i}_\mathrm{s}^k$ and the permanent-magnet flux linkage vector $\boldsymbol{\psi}_\mathrm{pm}^k$ (in Wb^2). The inductance matrix $\boldsymbol{L}_\mathrm{s}^k$ with stator inductances $L_\mathrm{s}^d > 0$, $L_\mathrm{s}^q > 0$ and mutual (cross-coupling) inductance $L_\mathrm{m} \neq 0$ is *symmetric* and *positive-definite* (i.e. $L_\mathrm{s}^d L_\mathrm{s}^q - L_\mathrm{m}^2 > 0$ [17]). If the anti-diagonal elements L_m of the inductance matrix $\boldsymbol{L}_\mathrm{s}^k$ are non-zero, a change in the d-axis current i_s^d imposes a change in the q-axis flux linkage ψ_s^q and vice versa. This effect is referred to as *magnetic cross-coupling*. Moreover, if the main-diagonal elements L_s^d and L_s^q have different values, i.e. $L_\mathrm{s}^d - L_\mathrm{s}^q \neq 0\,\mathrm{H}$, the (three-phase) stator flux linkage depends on the actual rotor position/angle, and the machine is said to be *anisotropic*. Fig. 2 illustrates the third quadrant (generator mode) of the flux linkage (3) of the simulated PMSM (see Sec. 3). Due to magnetic cross-coupling, the flux maps are slightly tilted. The electro-mechanical torque for such an anisotropic machine is given by[3]

$$m_\mathrm{m}(\boldsymbol{i}_\mathrm{s}^k) = \tfrac{3}{2}n_\mathrm{p}\,(\boldsymbol{i}_\mathrm{s}^k)^\top \boldsymbol{J}\boldsymbol{\psi}_\mathrm{s}^k \boldsymbol{i}_\mathrm{s}^k = \underbrace{\tfrac{3}{2}n_\mathrm{p}\,\psi_\mathrm{pm} i_\mathrm{s}^q}_{\text{(i)}} + \underbrace{\tfrac{3}{2}n_\mathrm{p}\,(L_\mathrm{s}^d - L_\mathrm{s}^q) i_\mathrm{s}^d i_\mathrm{s}^q}_{\text{(ii)}} + \underbrace{\tfrac{3}{2}n_\mathrm{p}\,L_\mathrm{m}\big((i_\mathrm{s}^q)^2 - (i_\mathrm{s}^d)^2\big)}_{\text{(iii)}}, \quad (4)$$

and can be split into three components: (i) permanent magnet torque, (ii) reluctance torque, and (iii) torque due to magnetic cross coupling (which is usually neglected [10]). Clearly, there exist infinitely many current vectors $\boldsymbol{i}_\mathrm{s}^k$ to produce the same torque (see (4) and/or Fig. 3).

2.2. Problem formulation

The MTPA optimization problem can be formulated as: *Find the minimum current magnitude* $\|\boldsymbol{i}_\mathrm{s}^k\|^2 = (\boldsymbol{i}_\mathrm{s}^k)^\top \boldsymbol{i}_\mathrm{s}^k$ *for a given reference torque* $m_\mathrm{m,ref}$ (see e.g. $m_\mathrm{m,ref}$ as in (17) in regime II), i.e.

$$\boldsymbol{i}_\mathrm{s,ref}^k = \mathrm{MTPA}(m_\mathrm{m,ref}, L_\mathrm{s}^d, L_\mathrm{s}^q, L_\mathrm{m}, \psi_\mathrm{pm}, \dots) := \arg\min_{\boldsymbol{i}_\mathrm{s}^k} \|\boldsymbol{i}_\mathrm{s}^k\|^2 \text{ such that } m_\mathrm{m}(\boldsymbol{i}_\mathrm{s}^k) = m_\mathrm{m,ref}.$$

[2] Note that a *constant* matrix $\boldsymbol{L}_\mathrm{s}^k$ is considered. Most publications deal with constant inductances L_s^d and L_s^q while the cross-coupling inductance L_m is neglected [9, 10, 12]. Future work will consider nonlinear flux linkages.
[3] For the sake of readability, the time-dependency will be omitted in the following. The factor 3/2 is due to an amplitude-correct Clarke transformation [18].

Journal of Physics: Conference Series **753** (2016) 112009 doi:10.1088/1742-6596/753/11/112009

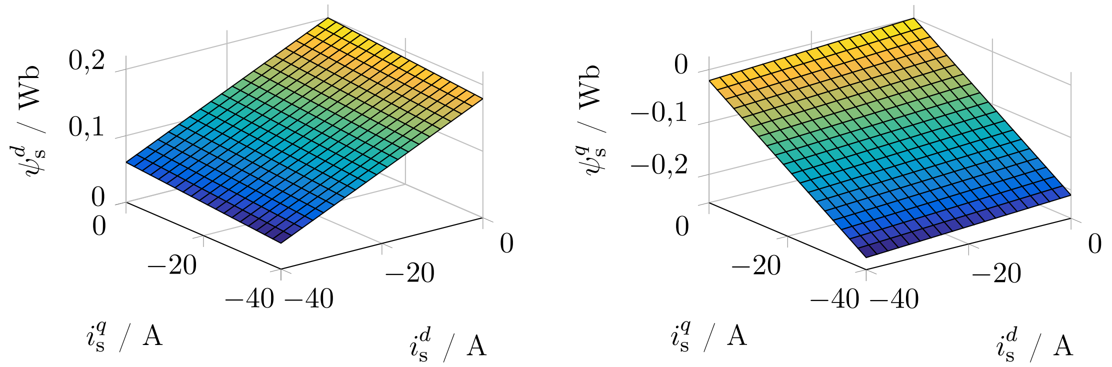

(a) *q-component* ψ_s^d *of the stator flux linkage.* (b) *q-component* ψ_s^q *of the stator flux linkage.*

Figure 2: *Flux linkage maps* (3) *of an anisotropic PMSM with parameters as in* (16).

Due to the equality constraint, the optimization problem can be rewritten as Lagrangian

$$\max_{(\boldsymbol{i}_s^k,\kappa)} \mathfrak{L}(\boldsymbol{i}_s^k,\kappa) \;\text{ where }\; \mathfrak{L}(\boldsymbol{i}_s^k,\kappa) := -(\boldsymbol{i}_s^k)^\top \boldsymbol{i}_s^k + \kappa\big[m_m(\boldsymbol{i}_s^k) - m_{m,ref}\big] \tag{5}$$

with Lagrangian multiplier $\kappa \in \mathbb{C} \setminus \{0\}$. Clearly, $(\boldsymbol{i}_s^k)^\top \boldsymbol{J}\boldsymbol{L}_s^k \boldsymbol{i}_s^k \overset{(3),(2)}{=} (\boldsymbol{i}_s^k)^\top \big[\frac{1}{2}(\boldsymbol{J}\boldsymbol{L}_s^k + \boldsymbol{L}_s^k\boldsymbol{J}^\top)\big]\boldsymbol{i}_s^k$ and $(\boldsymbol{i}_s^k)^\top \boldsymbol{J}\boldsymbol{\psi}_{pm}^k = (\boldsymbol{\psi}_{pm}^k)^\top \boldsymbol{J}^\top \boldsymbol{i}_s^k$. Then, by defining $\boldsymbol{I}_2 := \left[\begin{smallmatrix}1 & 0\\ 0 & 1\end{smallmatrix}\right]$,

$$\boldsymbol{T} := \tfrac{3}{4}n_p(\boldsymbol{J}\boldsymbol{L}_s^k + \boldsymbol{L}_s^k\boldsymbol{J}^\top) = \tfrac{3}{2}n_p \begin{bmatrix} -L_m & \frac{L_s^d - L_s^q}{2} \\ \frac{L_s^d - L_s^q}{2} & L_m \end{bmatrix} = \boldsymbol{T}^\top \;\text{ and }\; \boldsymbol{t} := \tfrac{3}{4}n_p \boldsymbol{J}\boldsymbol{\psi}_{pm}^k = \begin{pmatrix} 0 \\ \frac{3n_p\psi_{pm}}{4} \end{pmatrix}, \tag{6}$$

the machine torque can be expressed as $m_m(\boldsymbol{i}_s^k) \overset{(4),(6)}{=} (\boldsymbol{i}_s^k)^\top \boldsymbol{T}\boldsymbol{i}_s^k + 2\boldsymbol{t}^\top \boldsymbol{i}_s^k$ and the Lagrangian in (5) can be rewritten as quadric as follows

$$\begin{aligned} \mathfrak{L}(\boldsymbol{i}_s^k,\kappa) &\overset{(4)}{=} -(\boldsymbol{i}_s^k)^\top \boldsymbol{I}_2 \boldsymbol{i}_s^k + \kappa\big[\tfrac{3}{2}n_p\,(\boldsymbol{i}_s^k)^\top \boldsymbol{J}\boldsymbol{\psi}_s^k \boldsymbol{i}_s^k - m_{m,ref}\big] \\ &= (\boldsymbol{i}_s^k)^\top \Big[-\boldsymbol{I}_2 + \kappa\,\tfrac{3}{4}n_p(\boldsymbol{J}\boldsymbol{L}_s^k + \boldsymbol{L}_s^k\boldsymbol{J}^\top)\Big]\boldsymbol{i}_s^k + \kappa\,\tfrac{3}{2}n_p(\boldsymbol{\psi}_{pm}^k)^\top \boldsymbol{J}^\top \boldsymbol{i}_s^k - \kappa m_{m,ref} \\ &\overset{(6)}{=} (\boldsymbol{i}_s^k)^\top \big[-\boldsymbol{I}_2 + \kappa\,\boldsymbol{T}\big]\boldsymbol{i}_s^k + \kappa\,2\boldsymbol{t}^\top \boldsymbol{i}_s^k - \kappa\, m_{m,ref}. \end{aligned} \tag{7}$$

2.3. Analytical solution for the current references

To find the maximum of (5), it is sufficient to (i) set the gradient of (7) to zero and find its (optimal) solutions in $\boldsymbol{i}_s^{k,\star}$ and $\kappa^\star$ and (ii) check negative definiteness of the Hessian of (7). The gradient and the Hessian of (7) are given by

$$\boldsymbol{g}_{\mathfrak{L}}(\boldsymbol{i}_s^k,\kappa) := \left(\frac{\mathrm{d}\mathfrak{L}(\boldsymbol{i}_s^k,\kappa)}{\mathrm{d}(\boldsymbol{i}_s^k,\kappa)}\right)^\top = \begin{pmatrix} \frac{\mathrm{d}}{\mathrm{d}\boldsymbol{i}_s^k}\,\mathfrak{L}(\boldsymbol{i}_s^k,\kappa) \\ \frac{\mathrm{d}}{\mathrm{d}\kappa}\,\mathfrak{L}(\boldsymbol{i}_s^k,\kappa) \end{pmatrix} = \begin{pmatrix} 2\big[-\boldsymbol{I}_2 + \kappa\boldsymbol{T}\big]\boldsymbol{i}_s^k + \kappa\,2\boldsymbol{t} \\ (\boldsymbol{i}_s^k)^\top \boldsymbol{T}\boldsymbol{i}_s^k + 2\boldsymbol{t}^\top \boldsymbol{i}_s^k - m_{m,ref} \end{pmatrix} \in \mathbb{R}^3 \tag{8}$$

and

$$\boldsymbol{H}_{\mathfrak{L}}(\boldsymbol{i}_s^k,\kappa) := \left(\frac{\mathrm{d}^2\mathfrak{L}(\boldsymbol{i}_s^k,\kappa)}{\mathrm{d}(\boldsymbol{i}_s^k,\kappa)^2}\right)^\top = 2\begin{bmatrix} \big[-\boldsymbol{I}_2 + \kappa\boldsymbol{T}\big], & \boldsymbol{T}\boldsymbol{i}_s^k + \boldsymbol{t} \\ (\boldsymbol{i}_s^k)^\top \boldsymbol{T}^\top + \boldsymbol{t}^\top, & 0 \end{bmatrix} = \boldsymbol{H}_{\mathfrak{L}}(\boldsymbol{i}_s^k,\kappa)^\top \in \mathbb{R}^{3\times 3}, \tag{9}$$

respectively.

(i) Setting the gradient (8) to zero, i.e. $\boldsymbol{g}_{\mathfrak{L}}(\boldsymbol{i}_{\mathrm{s}}^{k,\star},\kappa) = \boldsymbol{0}_3$, and solving the first two rows for $\boldsymbol{i}_{\mathrm{s}}^{k,\star} = \boldsymbol{i}_{\mathrm{s}}^{k}$ yields

$$\boldsymbol{i}_{\mathrm{s}}^{k,\star}(\kappa) = -\big[-\boldsymbol{I}_2 + \kappa\boldsymbol{T}\big]^{-1}\kappa\boldsymbol{t} = -\begin{bmatrix} -1-\kappa\,\frac{3}{2}L_{\mathrm{m}}n_{\mathrm{p}} & \kappa\,\frac{3}{4}n_{\mathrm{p}}(L_{\mathrm{s}}^{d}-L_{\mathrm{s}}^{q}) \\ \kappa\,\frac{3}{4}n_{\mathrm{p}}(L_{\mathrm{s}}^{d}-L_{\mathrm{s}}^{q}) & -1+\kappa\,\frac{3}{2}L_{\mathrm{m}}n_{\mathrm{p}} \end{bmatrix}^{-1} \kappa \begin{pmatrix} 0 \\ \frac{3}{4}n_{\mathrm{p}}\psi_{\mathrm{pm}} \end{pmatrix}. \tag{10}$$

Inserting $\boldsymbol{i}_{\mathrm{s}}^{k,\star}(\kappa)$ into the last row of the gradient (8) gives a fourth-order polynomial

$$a_4\kappa^4 + a_3\kappa^3 + a_2\kappa^2 + a_1\kappa + a_0 = 0 \tag{11}$$

in κ with five coefficients $a_0, a_1, \ldots, a_4 \in \mathbb{R}$. The coefficients of (11) for the considered anisotropic PMSM model (2) depend on the machine parameters and are given by (details are omitted)

$$\begin{aligned}
&a_0 = -16m_{\mathrm{m,ref}}, \quad a_1 = -18n_{\mathrm{p}}^2(\psi_{\mathrm{pm}})^2, \\
&a_2 = m_{\mathrm{m,ref}}\left[36L_{\mathrm{m}}^2n_{\mathrm{p}}^2 + \left(3n_{\mathrm{p}}\left(L_{\mathrm{s}}^{d}-L_{\mathrm{s}}^{q}\right)\right)^2 + \frac{81}{2}L_{\mathrm{m}}n_{\mathrm{p}}^3(\psi_{\mathrm{pm}})^2\right], \qquad a_3 = 0, \qquad \text{and} \\
&a_4 = -\frac{81}{32}n_{\mathrm{p}}^4\left[2m_{\mathrm{m,ref}}\left(4L_{\mathrm{m}}^2 + (L_{\mathrm{s}}^{d}-L_{\mathrm{s}}^{q})^2\right)^2 + 3n_{\mathrm{p}}(\psi_{\mathrm{pm}})^2\left(4L_{\mathrm{m}}^2 + (L_{\mathrm{s}}^{d}-L_{\mathrm{s}}^{q})^2\right)\right].
\end{aligned}$$

Note that the resulting quartic is a *depressed* quartic (since $a_3 = 0$), which simplifies the calculation of its four roots $\kappa_1^\star, \ldots, \kappa_4^\star$. The four roots depend on the coefficients a_i, $i = 0, \ldots, 4$ only (and, hence, on machine parameters and reference torque only) and can be *computed analytically* e.g. by invoking *Ferrari's method* [16].

(ii) To obtain the optimal solution $(\boldsymbol{i}_{\mathrm{s}}^{k,\star}(\kappa^\star), \kappa^\star)$ of the optimization (*maximization*) problem (5), the Hessian matrix (9) must be *negative definite*. The root $\kappa^\star \in \{\kappa_1^\star, \ldots, \kappa_4^\star\}$, which renders the Hessian $\boldsymbol{H}_{\mathfrak{L}}(\boldsymbol{i}_{\mathrm{s}}^{k,\star}(\kappa^\star), \kappa^\star)$ negative definite, is the optimal Lagrangian multiplier. Therefore, the Hessian matrix must be evaluated for all $\kappa_i^\star$, $i = 1, \ldots, 4$ and checked for negative definiteness. This can be done by employing *Sylvester's criterion* [19, Prop. 8.2.8]: All leading principle minors of (9) must be negative, which is the case if (for details see the Appendix)

$$\left.\begin{array}{lllcll}
\text{(a)} & \kappa_i^\star & > -\frac{1}{\frac{3}{2}n_{\mathrm{p}}L_{\mathrm{m}}} & \Longrightarrow & -1-\frac{3}{2}n_{\mathrm{p}}L_{\mathrm{m}}\kappa_i^\star & < \ 0 \\
\text{(b)} & |\kappa_i^\star| & > \frac{1}{\frac{3}{2}n_{\mathrm{p}}\sqrt{\frac{1}{4}\left(L_{\mathrm{s}}^{d}-L_{\mathrm{s}}^{q}\right)^2+L_{\mathrm{m}}^2}} & \Longrightarrow & \det\big[-\boldsymbol{I}_2+\kappa_i^\star\boldsymbol{T}\big] & < \ 0.
\end{array}\right\} \tag{12}$$

Both conditions (a) and (b) must be satisfied simultaneously, hence the following must hold

$$\exists\kappa_i^\star \in \{\kappa_1^\star, \ldots, \kappa_4^\star\}: \qquad -\frac{1}{\frac{3}{2}n_{\mathrm{p}}L_{\mathrm{m}}} < \kappa^\star := \kappa_i^\star < -\frac{1}{\frac{3}{2}n_{\mathrm{p}}\sqrt{\frac{1}{4}\left(L_{\mathrm{s}}^{d}-L_{\mathrm{s}}^{q}\right)^2+L_{\mathrm{m}}^2}} < 0. \tag{13}$$

For generator (or motor mode) only *one* $\kappa^\star = \kappa_i^\star$ solves the optimization problem; which, finally, allows to compute the *unique* reference currents $\boldsymbol{i}_{\mathrm{s,ref}}^{k} := \boldsymbol{i}_{\mathrm{s}}^{k,\star}(\kappa^\star) = \mathrm{MTPA}(m_{\mathrm{m,ref}}, L_{\mathrm{s}}^{d}, L_{\mathrm{s}}^{q}, L_{\mathrm{m}}, \psi_{\mathrm{pm}}, \ldots)$ with $\boldsymbol{i}_{\mathrm{s}}^{k,\star}$ as in (10) and $\kappa^\star$ as in (13).

Remark 1: *As an alternative to evaluating the Hessian matrix,* (10) *can be evaluated for all four roots* $\kappa_1^\star, \ldots, \kappa_4^\star$*. The vector* $\boldsymbol{i}_{\mathrm{s}}^{k,\star}(\kappa_i^\star)$ *with the smallest magnitude is the optimal solution.*

Journal of Physics: Conference Series **753** (2016) 112009 doi:10.1088/1742-6596/753/11/112009

2.4. Torque and MTPA hyperbolas (implicit and explicit expressions)

To illustrate the effect of anisotropy and magnetic cross-coupling on the current reference computation, the plots of the torque hyperbola and the MTPA hyperbola in the current loci are helpful (see Fig. 3). For reference torque $m_{\mathrm{m,ref}}$, the torque hyperbola is implicitly given by

$$\mathrm{TRQ}(m_{\mathrm{m,ref}}) := \left\{ \boldsymbol{i}_{\mathrm{s}}^k \in \mathbb{R}^2 \;\middle|\; (\boldsymbol{i}_{\mathrm{s}}^k)^\top \boldsymbol{T} \boldsymbol{i}_{\mathrm{s}}^k + 2\,\boldsymbol{t}^\top \boldsymbol{i}_{\mathrm{s}}^k = 0 \right\}$$

where $\boldsymbol{T}$ and $\boldsymbol{t}$ are as in (6). Solving this quadric for i_{s}^q yields the explicit formula

$$\mathrm{TRQ}(i_{\mathrm{s}}^d, m_{\mathrm{m,ref}}) = \begin{cases} -\frac{(L_{\mathrm{s}}^d - L_{\mathrm{s}}^q) i_{\mathrm{s}}^d + \psi_{\mathrm{pm}}}{2L_{\mathrm{m}}} + \\ +\frac{\sqrt{[(L_{\mathrm{s}}^d - L_{\mathrm{s}}^q)^2 + 4L_{\mathrm{m}}^2](i_{\mathrm{s}}^d)^2 + 2\psi_{\mathrm{pm}}(L_{\mathrm{s}}^d - L_{\mathrm{s}}^q) i_{\mathrm{s}}^d + 4L_{\mathrm{m}}\frac{2m_{\mathrm{m,ref}}}{3p} + \psi_{\mathrm{pm}}^2}}{2L_{\mathrm{m}}} & , \; L_{\mathrm{m}} \neq 0 \\ \frac{m_{\mathrm{m,ref}}}{\frac{3}{2} n_{\mathrm{p}} \left[\psi_{\mathrm{pm}} + (L_{\mathrm{s}}^d - L_{\mathrm{s}}^q) i_{\mathrm{s}}^d\right]}, & , \; L_{\mathrm{m}} = 0 \end{cases} \tag{14}$$

as function of i_{s}^d which holds for all $i_{\mathrm{s}}^d \neq \psi_{\mathrm{pm}}/(L_{\mathrm{s}}^d - L_{\mathrm{s}}^q)$. Exemplary torque hyperbolas are plotted in Fig. 3 (see green lines). Note that, for $L_{\mathrm{m}} = 0$ and $L_{\mathrm{s}}^d = L_{\mathrm{s}}^q$ (isotropic case), the torque hyperbola becomes a horizontal line (see Fig. 3a).

To derive an expression for the MTPA hyperbola, in the first two rows of the gradient (8) (i.e. $2\big[-\boldsymbol{I}_2 + \kappa \boldsymbol{T}\big]\boldsymbol{i}_{\mathrm{s}}^k + \kappa\, 2\boldsymbol{t} = \boldsymbol{0}_2$), the Lagrangian multiplier κ can be eliminated. Solving this for κ and rearranging gives the implicit expression of the MTPA hyperbola as follows

$$\mathrm{MTPA} := \left\{ \boldsymbol{i}_{\mathrm{s}}^k \in \mathbb{R}^2 \;\middle|\; (\boldsymbol{i}_{\mathrm{s}}^k)^\top \begin{bmatrix} \frac{3}{4} n_{\mathrm{p}} (L_{\mathrm{s}}^d - L_{\mathrm{s}}^q) & \frac{3}{2} n_{\mathrm{p}} L_{\mathrm{m}} \\ \frac{3}{2} n_{\mathrm{p}} L_{\mathrm{m}} & -\frac{3}{4} n_{\mathrm{p}} (L_{\mathrm{s}}^d - L_{\mathrm{s}}^q) \end{bmatrix} \boldsymbol{i}_{\mathrm{s}}^k + \big(\tfrac{3}{4} n_{\mathrm{p}} \psi_{\mathrm{pm}},\, 0\big) \boldsymbol{i}_{\mathrm{s}}^k = 0 \right\}.$$

Solving this quadric for i_{s}^q yields the explicit expression of the MTPA hyperbola

$$\mathrm{MTPA}(i_{\mathrm{s}}^d) = \begin{cases} \frac{2L_{\mathrm{m}} i_{\mathrm{s}}^d \pm \sqrt{[(L_{\mathrm{s}}^d - L_{\mathrm{s}}^q)^2 + 4L_{\mathrm{m}}^2](i_{\mathrm{s}}^d)^2 + (L_{\mathrm{s}}^d - L_{\mathrm{s}}^q)\psi_{\mathrm{pm}} i_{\mathrm{s}}^d}}{L_{\mathrm{s}}^d - L_{\mathrm{s}}^q} & , \; L_{\mathrm{s}}^d \neq L_{\mathrm{s}}^q \\ (i_{\mathrm{s}}^d = 0) & , \; L_{\mathrm{m}} = 0 \;\wedge\; L_{\mathrm{s}}^d = L_{\mathrm{s}}^q. \end{cases} \tag{15}$$

In Fig. 3b, it can be clearly seen that, for a machine with $L_{\mathrm{m}} \neq 0$, neglecting the magnetic cross-coupling will have a significant effect on the shape of the MTPA hyperbola and, hence, on the current reference computation. The computed reference will not have a minimal magnitude.

3. Simulation results

For the upcoming simulations, a small-scale wind turbine system (SS-WTS) with a 17.7 kW PMSM is considered. The PMSM has rated torque $m_{\mathrm{m,rated}} = 49.3\,\mathrm{N\,m}$, rated speed $\omega_{\mathrm{m,rated}} = 360\,\frac{\mathrm{rad}}{\mathrm{s}}$ and the following electrical parameters

$$L_{\mathrm{s}}^d = 3.5\,\mathrm{mH},\; L_{\mathrm{s}}^q = 1.5 L_{\mathrm{s}}^d,\; L_{\mathrm{m}} = 0.15 L_{\mathrm{s}}^d,\; \psi_{\mathrm{pm}} = 0.2\,\mathrm{Wb},\; n_{\mathrm{p}} = 3 \;\text{ and }\; R_{\mathrm{s}} = 0.12\,\Omega. \tag{16}$$

Three different MTPA strategies are implemented:

- the proposed **MTPA** considering anisotropy and cross-coupling (i.e. $L_{\mathrm{s}}^d \neq L_{\mathrm{s}}^q$ and $L_{\mathrm{m}} \neq 0$, see **solid blue line** (——) in Fig. 4 and 5),
- the standard **MTPA**$(L_{\mathrm{m}}=0)$ considering anisotropy but neglecting cross-coupling (i.e. $L_{\mathrm{s}}^d \neq L_{\mathrm{s}}^q$ and $L_{\mathrm{m}} = 0$, see **dashed blue line** (- - - -) in Fig. 4 and 5) [10], and

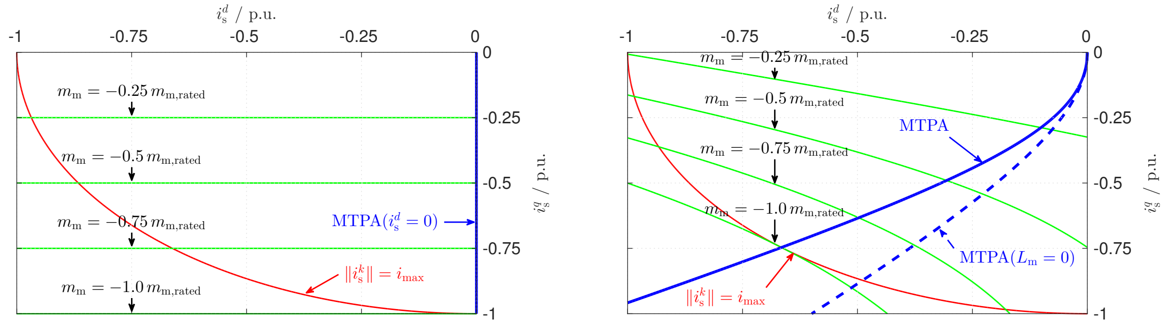

(a) *Isotropic machine with* $m_m(\boldsymbol{i}_s^k) = \frac{3}{2}\psi_{pm} i_s^d$.

(b) *Anisotropic machine with* $m_m(\boldsymbol{i}_s^k)$ *as in* (4).

Figure 3: *Generator mode current loci of an isotropic machine (with* $L_s^d = L_s^q$ *and* $L_m = 0$*) and an anisotropic machine with parameters as in* (16)*. The axes are normalized with respect to the maximal admissible current* i_{max} *(in* A*).*

- the simple **MTPA($i_s^d\!=\!0$)** usually used for isotropic machines with $i_{s,ref}^d = i_s^d = 0$ neglecting anisotropy and cross-coupling (i.e. $L_s^d = L_s^q$ and $L_m = 0$, see **dotted red line** (⋯⋯) in Fig. 4 and 5) [13].

Simulations have been conducted in Matlab/Simulink (R2016a) to compare the performance and the effects of the MTPA strategies on the efficiency of the electrical drive system and the overall small-scale wind turbine system. Moreover, the proposed MTPA considering anisotropy and cross-coupling was implemented by using the *analytical* solution and a conventional *numerical* solution (Newton-Raphson). Both solutions match with high accuracy (deviation $< 10^{-26}$), but the analytical solution was obtained 20 times faster than the numerical one. In the remainder, only the analytical solutions for the three MTPA strategies are implemented and discussed.

Remark 2: *Note that the proposed algorithm is applicable to any PMSM, PME-RSM or EESM with non-negligible anisotropy and magnetic cross-coupling independently of the machine's power rating. Small-scale machines tend to have a higher ratio of reluctance torque to permanent magnet torque (represented by (i) and (ii) in* (4)*, respectively) and, therefore, the application to small-scale wind turbine systems is discussed, since it illustrates better the efficiency gain of the proposed analytical MTPA strategy.*

3.1. Current loci and efficiency improvement of the electrical drive system

Fig. 3 shows the current loci (third quadrant/generator mode) of an isotropic PMSM (see Fig. 3a) and an anisotropic PMSM with parameters as in (16) (see Fig. 3b). Anisotropy and magnetic cross-coupling are *not* negligible and should be considered in the MTPA strategy. Neglecting L_m leads to an *incorrect* computation of the reference currents (see Fig. 3b) and, hence, higher losses (see Fig. 4b). For copper losses $P_{Cu} = \frac{3}{2} R_s \|\boldsymbol{i}_s^k\|^2$, friction losses $P_{fric} = \nu_f \omega_m^2$ and mechanical power $P_{mech} = m_m(\boldsymbol{i}_s^k)\omega_m$, the efficiencies[4] $\eta = (P_{mech} - P_{Cu} - P_{fric})/P_{mech} = 1 - (P_{Cu} + P_{fric})/P_{mech}$ are compared in *generator mode* for *different* speeds ω_m using the simple MTPA($i_s^d\!=\!0$), the conventional MTPA($L_m\!=\!0$) and the proposed MTPA (considering cross-coupling). As illustrated in Fig. 4, considering anisotropy *and* cross-coupling allows for a significant efficiency improvement differing for different machine speeds. The efficiency increase compared to the simple MTPA($i_s^d\!=\!0$) is measured by the *relative efficiency gain* (see Fig. 4c)

$$\Delta\eta := \eta(X) - \eta(\mathrm{MTPA}(i_s^d\!=\!0)) = \frac{P_{Cu}(\mathrm{MTPA}(i_s^d\!=\!0)) - P_{Cu}(X)}{P_{mech}} \text{ with } X \in \{\mathrm{MTPA}, \mathrm{MTPA}(L_m\!=\!0)\}.$$

[4] Iron losses are not considered. For WTS, the angular speed will (in most cases) not exceed the rated speed.

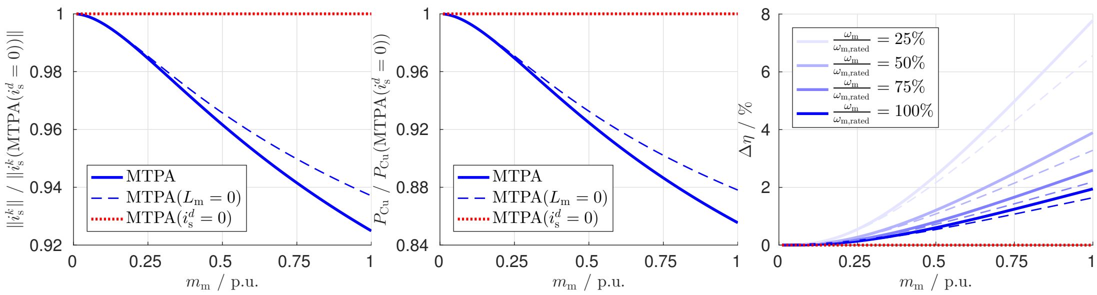

(a) *Current magnitude.* (b) *Copper losses.* (c) *Efficiency improvement.*

Figure 4: *Comparison of MTPA, MTPA($L_\mathrm{m}=0$) and MTPA($i_\mathrm{s}^d=0$) for parameters as in* (16) *(generator mode). The horizontal axes are normalized with respect to the rated machine torque $m_\mathrm{m,rated}$ (in* N m*).*

3.2. Overall small-scale wind turbine system (SS-WTS) with anisotropic PMSM

Now, three identical SS-WTSs with anisotropic PMSM (2) parametrized as in (16), gear ratio $g_\mathrm{r}=14.7$, inertia $\Theta=0.199\,\frac{\mathrm{kg}}{\mathrm{m}^2}$ and viscous friction coefficient $\nu_\mathrm{f}=5\cdot10^{-3}\,\frac{\mathrm{N\,m\,s}}{\mathrm{rad}}$ are implemented in Matlab/Simulink. The SS-WTS has turbine power $P_\mathrm{t}=c_\mathrm{p}(\lambda)P_\mathrm{w}$ (in W) and turbine torque $m_\mathrm{t}=P_\mathrm{t}\frac{g_\mathrm{r}}{\omega_\mathrm{m}}$ [18] where $P_\mathrm{w}=\frac{1}{2}\varrho\pi r_\mathrm{t}^2 v_\mathrm{w}^3$ (in W), $\varrho=1.293\,\frac{\mathrm{kg}}{\mathrm{m}^3}$, $r_\mathrm{t}=3.38\,\mathrm{m}$ and v_w (in $\frac{\mathrm{m}}{\mathrm{s}}$) are wind power, air density, turbine radius and wind speed, respectively. The power coefficient $c_\mathrm{p}(\cdot)$ from [20, Example III.2] with maximum $c_\mathrm{p}^\star := c_\mathrm{p}(\lambda^\star)=\max_\lambda c_\mathrm{p}(\lambda)=0.441$ and optimal tip speed ratio $\lambda^\star=6.91$ is used. For maximum power point tracking (MPPT) in region II (i.e. $v_\mathrm{w}\in[5,\,12]\frac{\mathrm{m}}{\mathrm{s}}$ for the simulations), the nonlinear turbine speed controller [18, 21]

$$m_\mathrm{m,ref}=-k_\mathrm{p}^\star\omega_\mathrm{m}^2+\nu_\mathrm{f}\omega_\mathrm{m}-\frac{\Theta_\mathrm{v}-\Theta}{T_\mathrm{v}}\xi \quad\text{where}\quad k_\mathrm{p}^\star := \frac{\varrho r_\mathrm{t}^5\pi}{2g_\mathrm{r}^3}\frac{c_\mathrm{p}(\lambda^\star)}{(\lambda^\star)^3}\quad\text{and}\quad \xi(s)=\left[1-\tfrac{1}{1+sT_\mathrm{v}}\right]\omega_\mathrm{m}(s) \tag{17}$$

with inertia compensation[5] [21, p. 482] and (viscous) friction feedforward compensation is implemented for all three SS-WTS. The underlying current control loops [17] are identical for all three SS-WTS. The only difference between the three SS-WTS is that the reference torque $m_\mathrm{m,ref}$ (controller output) is fed to one of the three introduced MTPA strategies (see above).

The simulation results are depicted in Fig. 5 (line colors are as introduced above). The wind speed $v_\mathrm{w}(\cdot)$ varies within the interval $[7,\,12]\frac{\mathrm{m}}{\mathrm{s}}$. Only the SS-WTS with the proposed MTPA (considering cross-coupling) achieves maximum power point tracking (MPPT) at steady state, since $\lambda\to\lambda^\star$ for all wind speeds (see second subplot in Fig. 5). For the SS-WTS with MTPA($i_\mathrm{s}^d=0$) and MTPA($L_\mathrm{m}=0$), the speed controller (17) does *not* guarantee MPPT; not even at steady state. Due to the *incorrect* current reference computation, the produced machine torque $m_\mathrm{m}\neq m_\mathrm{m,ref}$ differs from the reference torque (17) (see also [22]) and $\lambda\to\lambda^\star$ can *not* be established. Hence, the maximum turbine power $c_\mathrm{p}^\star P_\mathrm{w}$ can *not* be extracted, i.e. $P_\mathrm{t}=c_\mathrm{p}(\lambda)P_\mathrm{w}<c_\mathrm{p}^\star P_\mathrm{w}$. The relative extracted power ΔP_ext (normalized with respect to the maximum turbine power $c_\mathrm{p}^\star P_\mathrm{w}$) and the relative torque deviation Δm_m (normalized with respect to the reference torque (17)) of each SS-WTS can be computed by

$$\Delta P_\mathrm{ext} := \frac{(c_\mathrm{p}(\lambda)P_\mathrm{w}-P_\mathrm{Cu}-P_\mathrm{fric})-c_\mathrm{p}^\star P_\mathrm{w}}{c_\mathrm{p}^\star P_\mathrm{w}} \quad\text{and}\quad \Delta m_\mathrm{m} := \frac{m_\mathrm{m}-m_\mathrm{m,ref}}{m_\mathrm{m,ref}},$$

respectively. Δm_m and ΔP_ext are shown in the third and fourth subplot of Fig. 5, respectively. For example, for the SS-WTS with MTPA($i_\mathrm{s}^d=0$) at $v_\mathrm{w}=12\,\frac{\mathrm{m}}{\mathrm{s}}$, the relative torque deviation can reach more than 15% with a relative loss in extracted power of almost 8.5% .

[5] Note that $\xi\approx T_\mathrm{v}\frac{\mathrm{d}}{\mathrm{d}t}\omega_\mathrm{m}$ approximates the time derivative of the machine speed and $\Theta_\mathrm{v}<\Theta$ (in $\mathrm{kg\,m}^2$) is the desired reduced (virtual) inertia of the WTS. For the simulations, $\Theta_\mathrm{v}=\Theta/4$ and $T_\mathrm{v}=0.2\,\mathrm{s}$ were chosen.

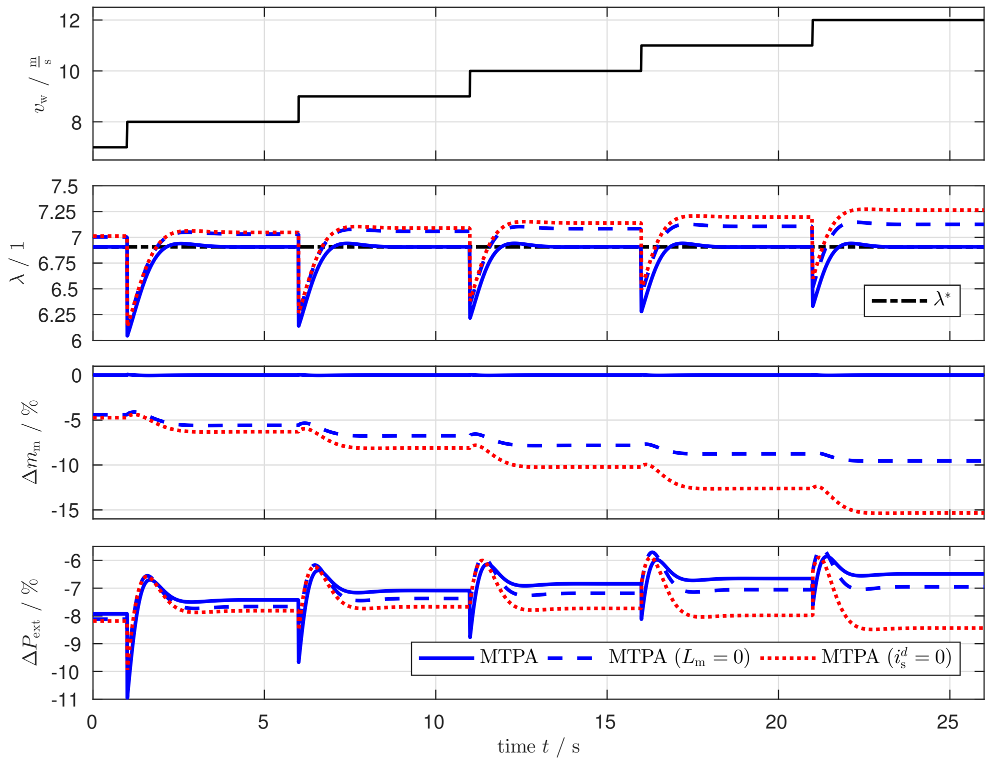

Figure 5: *Simulation results for a SS-WTS with anisotropic PMSM (parametrized as in* (16)*) operated in region II (maximum power point tracking) under (step-like) varying wind speeds* $v_w(\cdot) \in [7, 12]\,\frac{m}{s}$.

4. Conclusion

In this paper, an *analytical solution* for the Maximum-Torque-per-Ampere (MTPA) optimization problem has been derived for permanent-magnet synchronous machines with *anisotropy* and *magnetic cross-coupling*. The proposed MTPA strategy has been applied to a small-scale wind turbine system. The main contributions of this paper have been (i) the derivation of the analytical solution considering magnetic cross-coupling (which has not been done in literature before) and (ii) performance and efficiency comparisons with both, the conventional method (with zero direct current) and the state of the art MTPA strategy (neglecting magnetic cross-coupling). It has been shown that including the magnetic cross-coupling into the optimization problem can significantly increase the efficiency of the system (copper losses are reduced). Moreover, the analytical solution allows for an almost instantaneous computation of the optimal reference currents. Compared to the numerical Newton-Raphson method, the analytical solution converged to the correct solution 20 times faster. The proposed analytical MTPA strategy and its reference current computation can be adopted within already existing small-scale or large-scale wind turbine systems (WTSs) without any further modifications. Independently of the machine's power rating, the proposed solution can be applied to any permanent-magnet synchronous machine (PMSM), permanent-magnet-excited reluctance synchronous machine (PME-RSM) or electrically-excited synchronous machine (EESM) with non-negligible anisotropy and magnetic cross-coupling (see also Remark 2). Future work will focus on the extension of the analytical solution to nonlinear flux maps (i.e., when the inductances are functions of the stator currents).

Acknowledgement

This work is supported by the EU ITN AWESCO project funded by the European Union Commission under Marie Sklodowska-Curie ITN H2020 Ref.: 642682.

Journal of Physics: Conference Series **753** (2016) 112009 doi:10.1088/1742-6596/753/11/112009

Appendix

Note that, by defining

$$\boldsymbol{M}(\boldsymbol{i}_{\mathrm{s}}^k) := \begin{bmatrix} \boldsymbol{I}_2, & \big[-\boldsymbol{I}_2+\kappa\boldsymbol{T}\big]^{-1}(\boldsymbol{T}\boldsymbol{i}_{\mathrm{s}}^k+\boldsymbol{t}) \\ \boldsymbol{0}_2^\top, & 1 \end{bmatrix} \in \mathbb{R}^{3\times 3} \quad \text{with} \quad \det \boldsymbol{M}(\boldsymbol{i}_{\mathrm{s}}^k) = 1$$

and by invoking [19, Fact 2.16.2], the Hessian matrix

$$\boldsymbol{H}_{\mathfrak{L}}(\boldsymbol{i}_{\mathrm{s}}^k,\kappa) = 2\boldsymbol{M}(\boldsymbol{i}_{\mathrm{s}}^k)^\top \begin{bmatrix} \big[-\boldsymbol{I}_2+\kappa\boldsymbol{T}\big], & \boldsymbol{0}_2 \\ \boldsymbol{0}_2^\top, & -\big((\boldsymbol{i}_{\mathrm{s}}^k)^\top\boldsymbol{T}^\top+\boldsymbol{t}^\top\big)\big[-\boldsymbol{I}_2+\kappa\boldsymbol{T}\big]^{-1}\big(\boldsymbol{T}\boldsymbol{i}_{\mathrm{s}}^k+\boldsymbol{t}\big) \end{bmatrix} \boldsymbol{M}(\boldsymbol{i}_{\mathrm{s}}^k)$$

can be written as product of three matrices. Hence,

$$\det\big[\boldsymbol{H}_{\mathfrak{L}}(\boldsymbol{i}_{\mathrm{s}}^k,\kappa)\big] = -2\underbrace{\big((\boldsymbol{i}_{\mathrm{s}}^k)^\top\boldsymbol{T}^\top+\boldsymbol{t}^\top\big)\big[-\boldsymbol{I}_2+\kappa\boldsymbol{T}\big]^{-1}\big(\boldsymbol{T}\boldsymbol{i}_{\mathrm{s}}^k+\boldsymbol{t}\big)}_{=:\alpha\in\mathbb{R}} \cdot \det\big[-\boldsymbol{I}_2+\kappa\boldsymbol{T}\big],$$

which, with $\det \boldsymbol{M}(\boldsymbol{i}_{\mathrm{s}}^k) = \det \boldsymbol{M}(\boldsymbol{i}_{\mathrm{s}}^k)^\top = 1$ and $\det\big[-\boldsymbol{I}_2+\kappa\boldsymbol{T}\big] \overset{(12)}{<} 0$, implies that $\alpha = \|\boldsymbol{T}\boldsymbol{i}_{\mathrm{s}}^k+\boldsymbol{t}\|_{\boldsymbol{Q}}^2 < 0$ (a weighted norm with negative definite $\boldsymbol{Q} := \big[-\boldsymbol{I}_2+\kappa\boldsymbol{T}\big] < 0$) is negative for all non-zero vectors $\boldsymbol{T}\boldsymbol{i}_{\mathrm{s}}^k+\boldsymbol{t} \neq \boldsymbol{0}_2$. Inserting $\boldsymbol{i}_{\mathrm{s}}^k = \boldsymbol{i}_{\mathrm{s}}^{k,\star}(\kappa)$ with $\boldsymbol{i}_{\mathrm{s}}^{k,\star}(\kappa)$ as in (10) yields

$$\begin{aligned}
\boldsymbol{T}\boldsymbol{i}_{\mathrm{s}}^{k,\star}(\kappa)+\boldsymbol{t} &\overset{(10)}{=} -\kappa\boldsymbol{T}\big[-\boldsymbol{I}_2+\kappa\boldsymbol{T}\big]^{-1}\boldsymbol{t}+\boldsymbol{t} = -\big(-\boldsymbol{I}_2+\kappa\boldsymbol{T}\big[-\boldsymbol{I}_2+\kappa\boldsymbol{T}\big]^{-1}\big)\boldsymbol{t} \\
&= -\big(-\big[-\boldsymbol{I}_2+\kappa\boldsymbol{T}\big]\big[-\boldsymbol{I}_2+\kappa\boldsymbol{T}\big]^{-1}+\kappa\boldsymbol{T}\big[-\boldsymbol{I}_2+\kappa\boldsymbol{T}\big]^{-1}\big)\boldsymbol{t} \\
&= -\big(\big[\boldsymbol{I}_2\cancel{-\kappa\boldsymbol{T}}\big]+\cancel{\kappa\boldsymbol{T}}\big)\big[-\boldsymbol{I}_2+\kappa\boldsymbol{T}\big]^{-1}\boldsymbol{t} \\
&= -\big[-\boldsymbol{I}_2+\kappa\boldsymbol{T}\big]^{-1}\boldsymbol{t} \overset{(12)}{\neq} \boldsymbol{0}_2 \quad \text{for all} \quad \kappa=\kappa^\star \text{ with } \kappa^\star \text{ as in (12).}
\end{aligned}$$

References

[1] Polinder H, Ferreira J A, Jensen B B, Abrahamsen A B, Atallah K and McMahon R A 2013 *IEEE Journal of Emerging and Selected Topics in Power Electronics* **1** 174–185 ISSN 2168-6777

[2] Cardenas R, Pena R, Alepuz S and Asher G 2013 *IEEE Transactions on Industrial Electronics* **60** 2776–2798 ISSN 0278-0046

[3] Xiao S, Yang G, Zhou H and Geng H 2013 *IEEE Transactions on Industrial Electronics* **60** 2820–2832 ISSN 0278-0046

[4] Lopez J, Gubia E, Olea E, Ruiz J and Marroyo L 2009 *IEEE Transactions on Industrial Electronics* **56** 4246–4254 ISSN 0278-0046

[5] Nakamura Y, Kudo T, Ishibashi F and Hibino S 1995 *IEEE Trans. on Power Electron.* **10** 247–253

[6] Schmidt E 2014 *Proceedings of the Australasian Universities Power Engineering Conference* pp 1–6

[7] Ahrens U, Diehl M and Schmehl R (eds) 2013 *Airborne Wind Energy* Green Energy and Technologies (Berlin Heidelberg: Springer-Verlag)

[8] Mademlis C, Kioskeridis I and Margaris N 2004 *IEEE Transactions on Energy Conversion* **19** 715–723

[9] Cavallaro C, Di Tommaso A, Miceli R, Raciti A, Galluzzo G and Trapanese M 2005 *IEEE Trans. on Ind. Electron.* **52** 1153–1160

[10] Preindl M and Bolognani S 2015 *IEEE Trans. on Power Electron.* **30** 4524–4535

[11] Kim J, Jeong I, Nam K, Yang J and Hwang T 2015 *IEEE Trans. on Ind. Electron.* **62** 6151–6159

[12] Panaitescu R C and Topa I 1998 *Proceedings of the 6th International Conference on Optimization of Electrical and Electronic Equipments, 1998. OPTIM '98.* vol 2 (IEEE) pp 451–456

[13] Rahman M A, Vilathgamuwa D M, Uddin M N and Tseng K J 2003 *IEEE Trans. on Ind. Appl.* **39** 408–416 ISSN 0093-9994

[14] Ni R, Xu D, Wang G, Ding L, Zhang G and Qu L 2015 *IEEE Trans. on Ind. Electron.* **62** 2135–2143

[15] Mademlis C and Margaris N 2002 *IEEE Trans. on Ind. Electron.* **49** 1344–1347

[16] Ungar A 1990 *Computers & Mathematics with Applications* **19** 33 – 39 ISSN 0898-1221

[17] Hackl C M, Kamper M J, Kullick J and Mitchell J C 2016 *IEEE 25th International Symposium on Industrial Electronics (ISIE)*

[18] Dirscherl C, Hackl C and Schechner K 2015 *Elektrische Antriebe – Regelung von Antriebssystemen* ed Schröder D (Springer-Verlag) chap 24, pp 1540–1614

[19] Bernstein D S 2009 *Matrix Mathematics — Theory, Facts, and Formulas with Application to Linear System Theory* 2nd ed (Princeton and Oxford: Princeton University Press)

[20] Hackl C M 2015 *Proceedings of the 54th IEEE Conference on Decision and Control* pp 2005–2012

[21] Burton T, Sharpe D, Jenkins N and Bossanyi E 2001 *Wind Energy Handbook* (John Wiley & Sons)

[22] Hackl C and Schechner K 2016 *6th edition of the conference "The Science of Making Torque from Wind" (TORQUE 2016)* vol to be published in the open access Journal of Physics: Conference Series (JPCS) (München, Germany)